

Dynamics of a Rigid Rod in a Glassy Medium

ANGEL J. MORENO^{1,2} AND WALTER KOB¹

¹ *Laboratoire des Verres. Université de Montpellier II. Place E. Bataillon. CC 069. F-34095 Montpellier, France.*

² *Dipartimento di Fisica and INFN Udr and Center for Statistical Mechanics and Complexity. Università di Roma “La Sapienza”. Piazzale Aldo Moro 2. I-00185 Roma, Italy.*

PACS. 66.30.-h – Diffusion in solids.

PACS. 05.40.-a – Fluctuation phenomena, random processes, noise, and Brownian motion.

PACS. 64.70 Pf – Glass transitions.

Abstract. – We present simulations of the motion of a single rigid rod in a disordered static 2d-array of disk-like obstacles. The rotational, D_R , and center-of-mass translational, D_{CM} , diffusion constants are calculated for a wide range of rod length L and density of obstacles ρ . It is found that D_{CM} follows the behavior predicted by kinetic theory for a hard disk with an effective radius $R(L)$. A dynamic crossover is observed in D_R for L comparable to the typical distance between neighboring obstacles d_{nn} . Using arguments from kinetic theory and reptation, we rationalize the scaling laws, dynamic exponents, and prefactors observed for D_R . In analogy with the enhanced translational diffusion observed in deeply supercooled liquids, the Stokes-Einstein-Debye relation is violated for $L > 0.6d_{nn}$.

Lorentz gases are systems in which a *single* classical particle moves through a disordered array of static obstacles. They are used as simple models for the dynamics of a light particle in a disordered environment which presents a much slower dynamics. With increasing density of the obstacles, dynamic correlations and memory effects start to become important for the motion of the diffusing particle, and the system shows the typical features of the dynamics of supercooled liquids, such as a transition to a non-ergodic phase of zero diffusivity [1,2]. The theoretical description of the dynamics of the Lorentz gas is highly non-trivial since, e.g., the diffusion constant or the correlation functions are non-analytical functions of the density of obstacles [1,2].

Diffusing particles and obstacles are generally modeled as disks or spheres in two and three dimensions, respectively. In this Letter we use molecular dynamics simulations to investigate, at low and moderate densities, a generalization of the Lorentz gas, namely a model in which the diffusing particle is a rigid rod. In contrast to the usual models, this system has an orientational degree of freedom, which for sufficiently long rods is expected to be strongly slowed down by steric hindrance. Furthermore this system will allow to gain insight into the relaxation dynamics of a nonspherical probe molecule immersed in a simple liquid, an experimental technique that is used, e.g., in photobleaching experiments to study the dynamics of glass-forming liquids [3], or the investigation of the coupling between the rotational and translational degrees of freedom in such liquids [4].

In the following we will consider for the array of obstacles a homogeneous “glassy” configuration instead of the more usual random structure. In this way we avoid the effects induced by the very different length scales present in a completely random medium [5], and which

complicate the physical interpretation of the observed dynamic features. For simplicity, simulations have been done in two dimensions, reducing the degrees of freedom to a rotational and two translational ones. However, we think that the physical picture proposed here for the interpretation of the the obtained results is also valid in a three dimensional system.

The rigid rod, of mass M , was modeled as N aligned beads of equal mass $m = M/N$, with a bond length 2σ . The rod length is thus given by $L = (2N - 1)\sigma$. In order to obtain the glassy host medium, we equilibrated at a density $\rho = 0.77\sigma^{-2}$ and at temperature $T = \epsilon/k_B$ a two-dimensional array of soft disks interacting via a potential $V(r) = \epsilon(\sigma/r)^{12}$. This procedure produced an homogeneous liquid-like configuration. The latter was then permanently frozen and was expanded to obtain the desired density of obstacles, defined as $\rho = n_{\text{obs}}/l_{\text{box}}^2$, with n_{obs} the number of obstacles and l_{box} the length of the square simulation box used for periodic boundary conditions. The same soft-disk potential $V(r)$ was used for the interaction between the beads and the obstacles. For computational efficiency, $V(r)$ was truncated and shifted at a cutoff distance of 2.5σ . In the following, space and time will be measured in the reduced units σ and $(\sigma^2 m/\epsilon)^{1/2}$, respectively. The rod was equilibrated at $T = \epsilon/k_B$. After the equilibration, a production run was done at constant energy. For statistical average, runs were carried out for typically 600-1000 different realizations of the ensemble single rod-obstacles. Runs covered 10^6 time units, corresponding to $(1 - 5) \times 10^8$ time steps, depending on the step size used for the different rod lengths and densities. Run times were significantly longer than the relaxation times of the system.

Fig. 1 shows typical trajectories of the rod center-of-mass (CM) for $\rho = 10^{-2}$ and different rod lengths. A transition from a typical random walk for short rods to a polygonal-like structure for long ones is observed. The latter consists of nearly longitudinal motions inside corridors delimited by the neighboring obstacles, connected by vertices corresponding to regions where the rod changes from a corridor to another one. The very different nature of these trajectories suggest a change in the transport mechanism when increasing the rod length at constant ρ . Thus, while for short rods simple rotational and translational Brownian dynamics is expected, for long ones rotations and transversal translations are strongly hindered, and one has reptation-like motion inside tubes formed by neighboring obstacles and which gives rise to the nearly straight long paths observed in the trajectories.

In order to understand this change in the dynamics we will make use of kinetic theory and reptation arguments. Consider first the translational dynamics. We describe the rod by an “effective hard rod” formed by a rectangle of width 2σ and length $L - \sigma$ and two semi-circles of radius σ attached at both ends, leading to an effective rod length $L + \sigma$. This allows us to set the size of the obstacles to zero, i.e. to treat them as point particles. If ψ is the angle formed by the rod axis and the CM velocity, it is easy to see that the projection of the effective rod in the transversal direction is $2\sigma + (L - \sigma)\sin\psi$. Integration over all the orientations yields an average projection $2R$, with $R = (L + (\pi - 1)\sigma)/\pi$. The isotropic nature of the Brownian regime at low densities suggests to substitute the real system by an equivalent Lorentz gas of hard disks having this latter radius. Kinetic theory and mode coupling calculations for hard disks of radius R and mean velocity $\langle v \rangle$ in a 2d-medium with density of point obstacles ρ lead, in first order, to the following result, valid at low and moderate densities [1]:

$$D_{\text{CM}}/D_{\text{CM}}^0 = 1 + (32/9\pi)\rho^* \ln \rho^* \quad , \quad (1)$$

with the reduced density $\rho^* = \rho R^2$, and $D_{\text{CM}}^0 = 3\langle v \rangle/16\rho R$ is the low-density limit, corresponding to Brownian motion -i.e., no correlation between consecutive collisions. Since for a Maxwell-Boltzmann distribution the mean CM velocity of the rod is given by $\langle v \rangle = (\pi k_B T/2M)^{1/2}$, the corresponding low-density limit for the CM translational diffusion con-

stant of the rod, within the picture of equivalent hard disks of radius $R = (L + (\pi - 1)\sigma)/\pi$, is:

$$D_{\text{CM}}^0 = \frac{3}{16} \left(\frac{\pi^3 k_{\text{B}} T}{2M} \right)^{1/2} \frac{1}{\rho(L + (\pi - 1)\sigma)} \quad (2)$$

and D_{CM} is obtained from Eqs. (1) and (2) by taking $\rho^* = \rho(L + (\pi - 1)\sigma)^2/\pi^2$.

Points in Fig. 2a correspond to the ratio $D_{\text{CM}}/D_{\text{CM}}^0$ obtained from the simulations, where D_{CM} is calculated as the long-time limit of $\langle(\Delta r)^2\rangle/4t$, with $\langle(\Delta r)^2\rangle$ the mean squared CM displacement. Brackets denote the ensemble average. As can be seen in Fig. 2b, within the ρ - and L -range investigated, the D_{CM} investigated cover about 4 orders of magnitude. Also included in Fig. 2a, is the theoretical prediction given by Eqs. (1) and (2). A good agreement with the simulation data is obtained for reduced densities ρ^* smaller than $\xi_2 \approx 0.2$, thus showing that in that range, the picture of the equivalent hard disk is correct even quantitatively and in particular, the logarithmic corrections to D_{CM}^0 in Eq. (1) give account for the observed decrease of $D_{\text{CM}}/D_{\text{CM}}^0$ at intermediate values of ρ^* . Since the typical distance between neighboring obstacles, d_{nn} , is given by $d_{\text{nn}} = \rho^{-1/2}$, $\rho^* = \xi_2$ corresponds to a rod length $L \approx 1.4d_{\text{nn}}$, and to a diameter for the equivalent hard disk of $2R \approx 0.9d_{\text{nn}}$. For hard disks of this size, one has very strong correlation effects and the first order expansion in Eq. (1) is not valid any more [1]. Indeed the continuation of Eq. (1) to larger values of ρ^* leads to an unphysical increase of the ratio $D_{\text{CM}}/D_{\text{CM}}^0$ (see the theoretical curve in Fig. 2a). In contrast to this, the increase of this ratio observed in the simulation results *does* have a physical origin. (Note that this increase is found only in the ratio and that D_{CM} decreases with increasing ρ^* , see Fig. 2b.) However, it is not possible to rationalize this increase within the picture of equivalent hard disks of radius $R = (L + (\pi - 1)\sigma)/\pi$. Instead, reptation of the effective rod allows the system to stay ergodic, which would not be the case for hard disks at large ρ^* , and hence to increase the ratio beyond 1.0. We will give below evidence for reptation as the transport mechanism for large ρ^* .

For the case of the rotational dynamics, a calculation from first principles, that would require to take into account the interactions of the obstacles with all the beads forming the rod, is not straightforward. However, it is well-known that heuristic approximations in the framework of elementary kinetic theory [6], as the one we are going to discuss now, lead, *for very low densities*, i.e., in the Brownian regime, to correct results within a factor $O(1)$. For a given ensemble of n_0 rods with CM velocity v and angular velocity ω , we calculate $n(\theta)$, the number of rods that rotate a given angle θ without colliding. A differential equation for this quantity can be obtained by taking into account that the number of rods undergoing a collision between θ and $\theta + d\theta$ is $n(\theta)$ multiplied by the probability of a collision in $d\theta$. By taking advantage of the equivalent hard disk picture, such a probability can be obtained as ρ times the area swept by the equivalent hard disk, $2Rdx = 2(L + (\pi - 1)\sigma)dx/\pi$, where dx and $d\theta$ are related through $dx = vd\theta/\omega$. Thus we obtain the differential equation $n(\theta + d\theta) - n(\theta) = dn = -2n(\theta)\rho Rvd\theta/\omega$, and after integration, $n(\theta) = n_0 \exp(-2\rho Rv\theta/\omega)$. The mean angular free path between collisions is obtained as $\langle\theta\rangle = (1/n_0) \int dv f(v) \int f(\omega) d\omega \int_0^{n_0} \theta dn$, where $f(v)$ and $f(\omega)$ are the Maxwell-Boltzmann distributions at temperature T of the CM and angular velocities respectively. Integration leads to $\langle\theta\rangle = \langle\omega\rangle\langle 1/v\rangle/(2\rho R)$. For a Maxwell-Boltzmann distribution we have $\langle\omega\rangle = (2k_{\text{B}}T/\pi I)^{1/2}$, with I the moment of inertia of the rod, and $\langle 1/v\rangle = (\pi M/2k_{\text{B}}T)^{1/2}$. Therefore, from all these results, and the expression from kinetic theory for the rotational diffusion constant, $D_{\text{R}} = \langle\theta\rangle\langle\omega\rangle$, we obtain:

$$\frac{D_{\text{R}}I}{M^{1/2}[L + (\pi - 1)\sigma]} = \left(\frac{k_{\text{B}}T}{2\pi^3}\right)^{1/2} \frac{1}{\rho^*} . \quad (3)$$

D_{R} is determined from the simulation as the long time limit of $\langle(\Delta\phi)^2\rangle/2t$, with $\langle(\Delta\phi)^2\rangle$ the mean squared angular displacement. In Fig. 3 we show its dependence on ρ^* (left set of data points and left ordinate). The thick solid line for $\rho^* < \xi_1 \approx 0.04$ represents Eq. (3) and shows a good agreement with the simulation results. This value of $\rho^* = \xi_1$ corresponds to a rod length $L \approx 0.6d_{\text{nn}}$. As a further test of the validity of this heuristic approach, we can calculate the low-density limit D_{CM}^0 following the same arguments for the equivalent system of hard disks, leading to a decay rate for a displacement r , $n(r) = n_0 \exp(-2\rho Rr)$, a mean free path $l = (2\rho R)^{-1}$, and a diffusion constant $D_{\text{CM}} = l\langle v\rangle/2 = \langle v\rangle/4\rho R$, i.e., a factor which is only 4/3 larger than the rigorous result $D_{\text{CM}}^0 = 3\langle v\rangle/16\rho R$. In Fig. 3 a crossover to a different dynamic regime is observed around $\rho^* = \xi_1$. As can be seen in Fig. 2, this value of ρ^* corresponds to a decay of a 15% from the low-density limit of D_{CM} , again consistent with the breakdown of the picture of Brownian dynamics.

For the regime $\rho^* > \xi_1$ we now follow reptation arguments similar to those developed for solutions of rigid linear polymers [7]. Thus, we assume that at a given time, the hindrance effects induced by the neighboring obstacles result in the confinement of the rod in the center of a tube of width S and length $L + \sigma$ equal to that of the effective rod. We decompose the long-time rotational diffusion as a sum of elementary processes i , each one having a persistence time τ_i inside a tube, where the rod sweeps a typical angle Ω_i . The rotational diffusion constant is estimated as $D_{\text{R}} = \Omega^2/2\tau$, where the average values of Ω and τ are taken. Due to the homogeneous nature of the host medium, only a small dispersion is expected for Ω_i and τ_i , and the latter equation should be a reasonable approximation. The persistence time τ can be estimated as the time that the rod takes to cover its effective length $L + \sigma$. Once the rod has moved this distance, the old tube has been left and a new tube is defined by the new neighboring obstacles. Therefore, τ can be obtained as $\tau = (L + \sigma)^2/4D_{\text{CM}}^0$, with D_{CM}^0 the low-density limit given by Eq. (2), since we are referring to the translational dynamics of the rod *inside* the free space of the tube. On the other hand, the angle swept inside the tube can be estimated as $\Omega = 2S/(L + \sigma)$. Due to the homogeneous configuration of the host medium, the width S can be estimated as $S = d_{\text{nn}} - 2\sigma = \rho^{-1/2} - 2\sigma$, where the term 2σ is an excluded area effect due to the finite width of the effective rod. From all these results, $D_{\text{R}} = \Omega^2/2\tau$ follows the scaling law:

$$\frac{D_{\text{R}} \left(1 + \frac{\sigma}{L}\right)^4 M^{1/2} L}{(1 - 2\rho^{1/2}\sigma)^2 \left(1 + \frac{(\pi-1)\sigma}{L}\right)^3} = \left(\frac{9k_{\text{B}}T}{8\pi^5}\right)^{1/2} \frac{1}{(\rho^*)^2} . \quad (4)$$

A good agreement with the simulation data is obtained, as shown by the thick solid line in Fig. 3 for $\rho^* > \xi_1 \approx 0.04$. Only a small, though systematic, deviation is observed at the largest values of ρ^* , suggesting that in this range the model is somewhat oversimplified. Except for these largest values, the agreement is particularly good for $\rho^* > \xi_2 \approx 0.2$, i.e., for the range where reptation was suggested as mechanism of ergodicity restoring for the translational motion. For $\xi_1 < \rho^* < \xi_2$, corresponding to a rod length $0.6d_{\text{nn}} < L < 1.4d_{\text{nn}}$, reptation also gives a reasonable description of the simulation data, although a more detailed theory might be required to describe this crossover regime.

It must be stressed that there is no functional continuity between Eqs. (3) and (4) and hence a more rigorous model should be introduced to obtain a unified description at both sides of the crossover point $\rho^* = \xi_1$. Nevertheless, we find that the curves for D_{R} predicted

by (3) and (4) actually cross at a value $\rho^* = \xi_{\text{co}}$ in agreement with the value of $\xi_1 \approx 0.04$ obtained from the simulations. It is straightforward to see that this common value is given by $\xi_{\text{co}} = \pi^{-2} \{1 + (\pi - 1)(\sigma/L)\}^2 \{2(\sigma/L) + (2M/3\pi I)^{1/2} (1 + (\sigma/L)^2 L)\}^{-2}$. This expression can be simplified by taking into account that, except for the highest investigated densities, the data in the reptation regime fulfill the condition $\sigma \ll L$ and therefore one can make the approximation $I = ML^2/12$. Using these two approximations we obtain for ξ_{co} the result $\rho^* = (8\pi)^{-1} \approx 0.04$, in agreement with the observed value of ξ_1 . From all these results, at this point it can be concluded that Brownian motion and reptation are the transport mechanisms respectively below and above $\rho^* = \xi_1$, the crossover taking place when the rod length is comparable to the typical distance between neighbouring obstacles. It is also noteworthy of remark that a consistent description has been achieved without any fit parameter.

Some insight about the coupling between the rotational and translational degrees of freedom can be obtained by investigating the validity of the Stokes-Einstein-Debye (SED) relation [8] $D_{\text{CM}}\tau_R = c$, where c is a constant and τ_R is the rotational relaxation time. We define this latter quantity as the time at which the correlation function $\langle \cos \Delta\phi(t) \rangle$ has decayed to $1/e$. In the limit of small ρ^* , where collisions are infrequent, one expects that the rod performs several full rotations between two consecutive collisions. In this case, the physical mechanism for the angular decorrelation is not the collisions but the free rotation of the rod between them. Therefore, in this limit τ_R can be calculated from the relation $\cos(\langle \omega \rangle \tau_R) = 1/e$, leading to $\tau_R = (\pi I/2k_B T)^{1/2} \cos^{-1}(1/e)$. A good agreement of this latter equation with the simulation data has been obtained for $\rho^* < \xi_1$, confirming the validity of the hypothesis (see Ref. [5]). Then, together with the low-density limit of D_{CM} given by Eq. (2), we obtain the following scaling law for the SED-relation:

$$D_{\text{CM}}^0 \tau_R \rho [L + (\pi - 1)\sigma] (M/I)^{1/2} = (3\pi^2/32) \cos^{-1}(1/e) \quad . \quad (5)$$

As shown in Fig. 4, the simulation data follow nicely this equation for $\rho^* < \xi_1$, i.e., for $L < 0.6d_{\text{nn}}$. Data for $\xi_1 < \rho^* < \xi_2$ are systematically below the constant value $(3\pi^2/32) \cos^{-1}(1/e)$, showing that the SED-relation is no more fulfilled in this range of ρ^* (the reason for this is the presence of the logarithmic correction given in Eq. (1)). Finally, a crossover to a power law $\sim (\rho^*)^{2.4}$ is obtained at $\rho^* = \xi_2$. (Note that presently we do not have an explanation for this power-law.) Thus, the SED-relation is clearly violated for rods that are significantly longer than d_{nn} , in analogy with the phenomenon of enhanced translational diffusion observed in supercooled liquids -with temperature as control parameter-, close to the glass transition [9], where the value of c increases with decreasing temperature, and that is explained by the different averaging of the rotational and translational degrees of freedom [10]. This interpretation is clearly evidenced by the trajectory of the center-of-mass for $L = 59$ in Fig. 1 and the picture of reptation at large values of ρ^* , where due to steric hindrance, the rod is able to perform only small rotations while it moves along nearly straight long paths. In this way, reptation leads to an enhancement of the translational decorrelation in comparison with the rotational one.

In summary, we have shown that arguments from kinetic theory and reptation are able to give a very good account for the translational and rotational dynamics of the considered generalization of the Lorentz gas. In particular the analysis show that in this system the violation of the Stokes-Einstein-Debye relation is due to the breakdown of the isotropy of the rotational dynamics, a result that will be useful for the interpretation of the experimental findings of this violation.

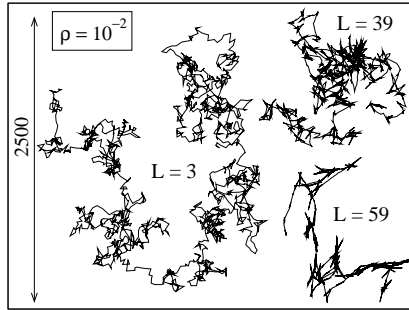


Fig. 1 – Typical trajectories of the rod CM at $\rho = 10^{-2}$, for $L = 3, 39$ and 59 . The simulation time is $t_{\text{sim}} = 10^6$, with a time interval of 500 between consecutive plotted points. The arrow indicates the length scale. Note that for the sake of clarity the obstacles are not shown.

We thank E. Frey for useful discussions. A.J.M. acknowledges a postdoctoral grant from the Basque Government. Part of this work was supported by the EC Human Potential Program under contract HPRN-CT-2002-00307, DYGLAGEMEM.

REFERENCES

- [1] GÖTZE W., LEUTHEUSSER E. AND YIP S., *Phys. Rev. A*, **23** (1981) 2634; *ibid.*, **24** (1981) 1008.
- [2] BRUIN C., *Phys. Rev. Lett.*, **29** (1972) 1670; MASTERS A. AND KEYES T., *Phys. Rev. A*, **26** (1982) 2129; BINDER P. M. AND FRENKEL D., *Phys. Rev. A*, **42** (1990) R2463.
- [3] CICERONE M. T., BLACKBURN F. R. AND EDIGER M. D., *J. Chem. Phys.*, **102** (1995) 471; CICERONE M. T., AND EDIGER M. D., *J. Chem. Phys.*, **103** (1995) 5684.

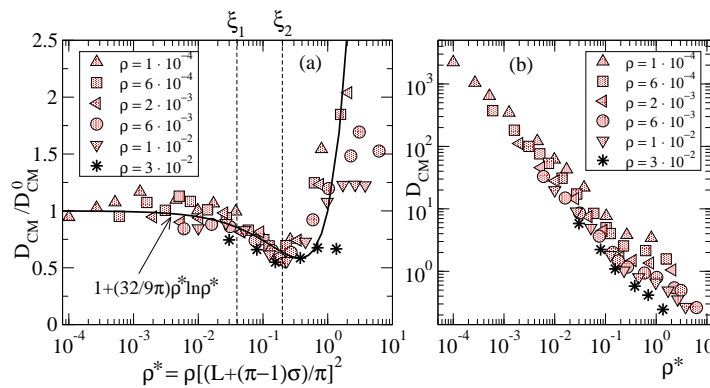


Fig. 2 – (a): Ratio between the CM translational diffusion constant D_{CM} obtained from the simulations and the low-density limit D_{CM}^0 for the equivalent hard disk (symbols). The solid curve corresponds to the theoretical prediction of kinetic theory for the equivalent hard disk at low and moderate densities, see Eq. (1). (b): CM translational diffusion constant vs. the reduced density.

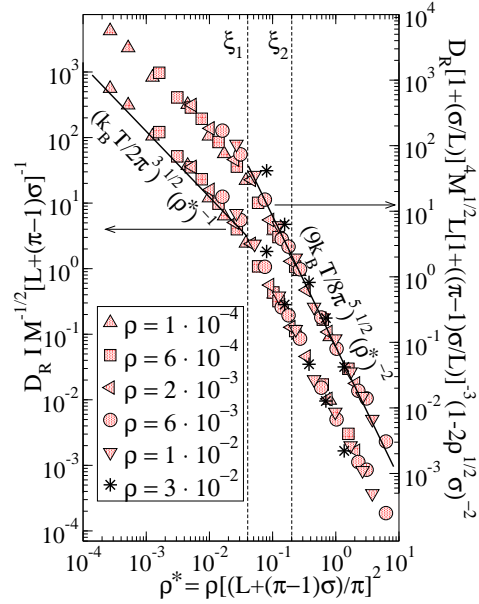


Fig. 3 – Scaling laws for D_R . A double- y representation is shown for clarity. Points are simulation data. Thick solid lines correspond to the theoretical predictions for Brownian and reptation dynamics (see text).

- [4] ANDREOZZI L., DI SCHINO A., GIORDANO M. AND LEPORINI D., *Europhys. Lett.*, **38** (1997) 669; TASHIN A., TORRE R., RICCI M., SAMPOLI M., DREYFUS C. AND PICK R. M., *Europhys. Lett.*, **56** (2001) 407.
- [5] MORENO A. J. AND KOB W., *J. Chem. Phys.*, **121** (2004) 380.
- [6] MCQUARRIE D. A., *Statistical Physics* (University Science Books, Sausalito, CA, USA) 2000.
- [7] DOI M., *J. Physique*, **36** (1975) 607; DOI M. AND EDWARDS S. F., *J. Chem. Soc., Faraday Trans.*, **74** (1978) 560.
- [8] EGELSTAFF P. A., *An Introduction to the Liquid State* (Oxford University Press, Oxford,

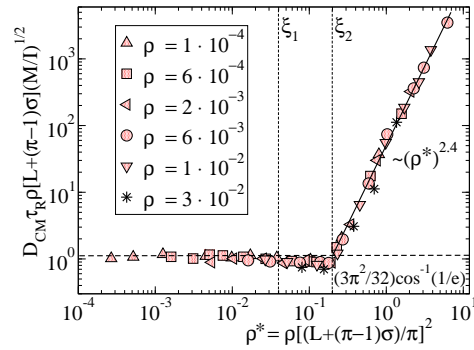


Fig. 4 – Scaling law for the product $D_{CM}\tau_R$ and violation of the SED relation at large ρ^* . The dashed line marks the theoretical constant value $(3\pi^2/32)\cos^{-1}(1/e)$ (see text). The solid line in the large- ρ^* regime is a fit to a power law.

U.K.) 1994.

- [9] FUJARA F., GEIL B., SILLESCU H. AND FLEISCHER G., *Z. Phys. B*, **88** (1992) 195;
EDIGER M.D., *Ann. Rev. Phys. Chem.*, **51** (2000) 99.
- [10] STILLINGER F. H. AND HODGDON J. A., *Phys. Rev. E*, **50** (1994) 2064.